




Geodesic Trajectories and Photon Sphere Analysis of Magnetically Charged Black Holes in Nonlinear Electrodynamics

Hira Waseem,^{1,*} Nikko John Leo S. Lobos ^{2,†} Ali Övgün ^{3,‡} and Reggie C. Pantig ^{4,§}

¹*Department Of Physics, Quaid-I-Azam University, Islamabad 45320, Pakistan.*

²*Electronics Engineering Department, University of Santo Tomas, España Blvd, Sampaloc, Manila, 1008 Metro Manila*

³*Physics Department, Eastern Mediterranean University, Famagusta, 99628 North Cyprus via Mersin 10, Turkiye.*

⁴*Physics Department, Mapúa University, 658 Muralla St., Intramuros, Manila 1002, Philippines*

(Dated: February 7, 2025)

In this paper, we investigate the gravitational lensing properties of magnetically charged black holes within the framework of nonlinear electrodynamics. We derive the deflection angle and examine the influence of the nonlinear electrodynamics parameter ξ on light bending. Initially, we employ a geometric approach based on the Gauss–Bonnet theorem to analyze the gravitational deflection of both null and timelike particles. This method encapsulates the global characteristics of the lensing effect in an elegant manner. In the subsequent part of the work, we explore the impact of nonlinear electromagnetic corrections on the black hole shadow. Using numerical techniques, we study the behavior of the photon sphere and demonstrate that a reduction in the photon sphere radius leads to a correspondingly smaller shadow. We compare these results with those for the Schwarzschild and Reissner–Nordström black holes, highlighting the distinctive features introduced by nonlinear electrodynamics. Furthermore, we examine the strong deflection limit for light trajectories near these black holes, focusing on the roles of both the magnetic charge Q and the nonlinear parameter ξ . Our analysis reveals that the combined effects of Q and ξ enhance the strong deflection angle, resulting in a more pronounced lensing effect than that predicted by the classical Reissner–Nordström solution. These findings suggest that the nonlinear interactions may provide a potential observational signature for identifying NED black holes.

PACS numbers: 95.30.Sf, 04.70.-s, 97.60.Lf, 04.50.+h

Keywords: Black holes; Nonlinear electrodynamics; Weak deflection angle; Shadow; Null geodesics.

I. INTRODUCTION

A longstanding question in differential geometry has been whether, for a given metric $g_{\mu\nu}(x)$, one can find a coordinate system in which the metric components are globally constant. This intriguing problem, which captivated many mathematicians in the past [1], was resolved by Riemann in 1861 [2]. Riemann showed that any coordinate transformation must preserve the distance between neighboring points a condition that is encoded in the Riemann curvature tensor, a fourth-rank tensor essential for characterizing the intrinsic geometry of a manifold. After 1915, Einstein's revolutionary interpretation of gravity transformed our understanding of the phenomenon. Gravity was no longer viewed as a conventional force but as a manifestation of the curvature of spacetime [3–5]. One of the enduring challenges in modern physics is the unification of quantum field theory with general relativity into a coherent theory of quantum gravity. In relativistic astrophysics, the deflection angle of particles moving in a gravitational field plays a crucial role. When the size of a particle is negligible compared to the gravitational system, its motion can be accurately described as a geodesic path representing the shortest distance between two points in curved spacetime. The boundedness or unboundedness of a particle's orbit depends on its kinematical and dynamical parameters, such as energy and angular momentum. Notably, massless particles like photons follow unbounded trajectories, and their paths have been studied extensively.

The bending of light was famously confirmed in 1919 during a solar eclipse by Dyson, Eddington, and Davidson [6], marking a cornerstone in astrophysics and cosmology as well as a pivotal experimental validation of general relativity. This phenomenon, now known as gravitational lensing, was predicted long before its observation its early theoretical suggestion even dating back to Soldner in 1801. Gravitational lensing not only reveals the presence of massive objects but also provides a powerful means to study exotic structures such as black holes and wormholes [7–15]. Gravitational lensing is especially versatile because the deflection angle of a light ray is determined by the gravitational field, which itself is governed by the stress-energy tensor of the matter distribution. Once the deflection angle is expressed as a function of the impact parameter,

* hirawaseem633@gmail.com

† nslobos@ust.edu.ph

‡ ali.ovgun@emu.edu.tr

§ rcpantig@mapua.edu.ph

the lensing effect reduces to a geometrical problem. This approach has been employed, for example, to determine the Hubble constant and the cosmic density parameter [16, 17]. In the framework of general relativity, a light ray passing by a spherical mass M at a minimum distance b is deflected by the so-called Einstein angle

$$\hat{\alpha} = \frac{4GM}{c^2 b} = \frac{2R_s}{b},$$

where $R_s = \frac{2GM}{c^2}$ is the Schwarzschild radius [18, 19].

In 2008, G. W. Gibbons and M. C. Werner introduced a novel geometrical approach to gravitational lensing by deriving the deflection angle from the Gaussian curvature of the optical metric. This method exploits the global properties of the deflection angle and employs the Gauss-Bonnet theorem, which elegantly links the intrinsic differential geometry of a surface with its topology. In their pioneering work, Gibbons and Werner applied this technique to analyze the deflection of photons in static, spherically symmetric spacetimes. Subsequently, the same method was adapted to determine the deflection angle for the optical metric of a gravitational lens modeled as a static, spherically symmetric, perfect non-relativistic fluid [20]. In 2012, by utilizing the Randers optical metric, Werner further extended this approach to study the deflection of massless particles specifically, photons in time-independent, axially symmetric (stationary axially symmetric) spacetimes. Werner applied this method to two examples of non-asymptotically flat spacetimes to suggest distance-dependent corrections: one case being the Kottler (Schwarzschild-de Sitter) solution to the Einstein equations, and the other an exact solution in Weyl conformal gravity [21]. Subsequently, a series of studies have employed the Gauss-Bonnet theorem (GBT) to determine the deflection angle [22–48]. However, the conventional treatment of boundless orbits assuming that both the source and observer are located at infinite distances from the lensing mass has been met with criticism. Some researchers argued that finite-distance corrections to the deflection angle should be incorporated when analyzing light propagation in asymptotically curved spacetimes. In response, Rindler and Ishak proposed a definition for the finite-distance deflection angle of light in the special case where the lens, receiver, and source are collinear [49]. Although this proposal received some criticism [50–52], a finite-distance deflection angle formulation based on the GW method was later introduced by Ishihara et al. [23], which has since gained widespread acceptance; the infinite-distance deflection angle can then be recovered as a limiting case. More recently, Li et al. employed the Jacobi-Maupertuis-Randers-Finsler metric in conjunction with the GB theorem to explore finite-distance effects on the deflection of heavy particles in time-independent, axially symmetric spacetimes [53–55]. Additionally, Arakida examined the deflection angle in the finite region by considering a vacuum solution [56], and Takizawa et al. investigated light deflection in asymptotically curved spacetimes using non-inertial circular orbits [57]. In this research, a geometric approach is employed to first derive the radius of the circular orbit for a particle, and then the Gauss-Bonnet theorem is applied to calculate its deflection angle.

In this work, we are also motivated to investigate the effects of nonlinear electrodynamics on black hole shadows. The black hole shadow represents a critical aspect of black hole physics, offering an observable manifestation of the event horizon. It is produced by the region where light is unable to escape the black hole's gravitational pull, thereby creating a dark silhouette against the luminous background of the surrounding accretion disk.

Pioneering studies on this phenomenon were conducted by Jean-Pierre Luminet in the late 1970s [58], who established the theoretical framework for visualizing black hole shadows by demonstrating how gravitational bending of light produces such distinct silhouettes. This theoretical foundation was spectacularly confirmed by the Event Horizon Telescope collaboration, which in 2019 captured the first image of a black hole shadow in the M87 galaxy [59–61] and later in the Milky Way galaxy in 2022 [62–64]. Such empirical evidence not only validates general relativity under extreme gravitational conditions but also marks a pivotal moment in observational astrophysics.

The study of black hole shadows is crucial for several reasons. It provides a direct test of gravitational theories in regions of intense curvature, offers insights into the behavior of matter (and even dark matter or other cosmological background parameters) as well as radiation near the event horizon [65–74], and enables the precise measurement of key black hole parameters such as mass, spin, and those emerging from alternative theories of gravity [75–90]. Consequently, black hole shadows serve as a unique diagnostic tool in probing the fundamental physics of gravity in its most extreme regimes.

Gravitational lensing in the strong deflection limit where light trajectories pass extremely close to the photon sphere provides a powerful means to probe the interplay between electromagnetic fields and gravity in high-energy astrophysical environments [91–94]. Although the weak deflection angle has been extensively studied in various black hole spacetimes, the strong deflection regime is particularly relevant for near-horizon physics, where deviations from general relativity become most pronounced. In the case of nonlinear electrodynamic (NED) magnetic black holes, the presence of nonlinear electromagnetic fields alters both the photon sphere radius and the critical impact parameter, leading to measurable differences in light bending.

This paper is organized as follows. In Section II, we review the magnetically charged black holes in nonlinear electrodynamics then in Section III, we introduce the geometric approach for understanding spacetime geodesics and detail the application of the Gauss-Bonnet theorem to derive the gravitational deflection angle. In Section IV, we calculate the strong deflection angle of photons. Section V is devoted to calculating the photon sphere radius and shadow radius. Finally, in Section VI we summarize our findings.

II. MAGNETICALLY CHARGED BLACK HOLES IN NONLINEAR ELECTRODYNAMICS

The action of Einstein's non-linear electrodynamics (NED) which is the Linearized Maxwell's theory in the weak field domain is written as,

$$S = \int d^4x \sqrt{-g} \left(\frac{\mathcal{R}}{16\pi} + \mathcal{L}(\mathcal{F}) \right), \quad (1)$$

where \mathcal{R} stands for the Ricci scalar, $G = 1$ (Gravitational constant) and $\mathcal{L}(\mathcal{F})$ is given as [95]

$$\mathcal{L} = -\varepsilon(\mathcal{F}) \mathcal{F}, \quad (2)$$

where

$$\varepsilon(\mathcal{F}) = \frac{16 \left(3\sqrt{2\mathcal{F}} + \xi \left(\xi + \sqrt{\xi^2 + 4\sqrt{2\mathcal{F}}} \right) \right)}{3 \left(\xi + \sqrt{\xi^2 + 4\sqrt{2\mathcal{F}}} \right)^4}, \quad (3)$$

where ξ represents the positive constant parameter. If ξ is small then,

$$\varepsilon(\mathcal{F}) \simeq 1 - \frac{4}{3} \frac{\sqrt[4]{2}}{\sqrt[4]{\mathcal{F}}} \xi + \left(\frac{\sqrt[4]{2}}{\sqrt[4]{\mathcal{F}}} \right)^2 \xi^2 + \mathcal{O}(\xi^3). \quad (4)$$

where this \mathcal{F} is electromagnetic tensor, $\frac{1}{4} F_{\mu\nu} F^{\mu\nu}$. Einstein NED equation takes the following form after the variation of action, Eq. (1) w.r.t NED energy-momentum tensor,

$$G_{\mu}^{\nu} = 8\pi T_{\mu}^{\nu}. \quad (5)$$

where T_{μ}^{ν} is

$$T_{\mu}^{\nu} = \frac{1}{4\pi} \left(\mathcal{L} \delta_{\mu}^{\nu} - \mathcal{L}_{\mathcal{F}} \mathcal{F}_{\mu\lambda} \mathcal{F}^{\nu\lambda} \right). \quad (6)$$

energy-momentum tensor. Maxwell's NED equations are yielded in the result of variation of action w.r.t gauge fields written as

$$d \left(\mathcal{L}_{\mathcal{F}} \tilde{\mathbf{F}} \right) = 0. \quad (7)$$

where this $\tilde{\mathbf{F}}$ is the dual electromagnetic field tensor,

$$\mathbf{F} = \frac{1}{2} F_{\mu\nu} dx^{\mu} \wedge dx^{\nu}. \quad (8)$$

Considering a magnetic monopole located at the origin with the field to form,

$$\mathbf{F} = Q \sin \theta d\theta \wedge d\phi. \quad (9)$$

The tt component of Eq. (6) gives,

$$\frac{r f'(r) + f(r) - 1}{r^2} = - \frac{4B^3 \left(2\xi^2 + 2\xi \sqrt{\xi^2 + 2B} + 3B \right)}{3 \left(\xi + \sqrt{\xi^2 + 2B} \right)^4}. \quad (10)$$

where $B = \frac{Q}{r^2}$ is the radial component of the magnetic field of the magnetic pole $Q > 0$. The exact solution of the Eq. (10) is [95],

$$f(r) = 1 - \frac{2M}{r} + \frac{Q^2}{r^2} - 2Q\xi^2 - \frac{2\xi^4 r^2}{9} - \frac{4}{3} \frac{Q^{\frac{3}{2}} \xi \sqrt{2}}{r} \times \ln \left(\frac{4Q + 2\sqrt{2Q} \sqrt{\xi^2 r^2 + 2Q}}{r} \right) + \frac{2\xi \sqrt{\xi^2 r^2 + 2Q} (\xi^2 r^2 + 8Q)}{9r}. \quad (11)$$

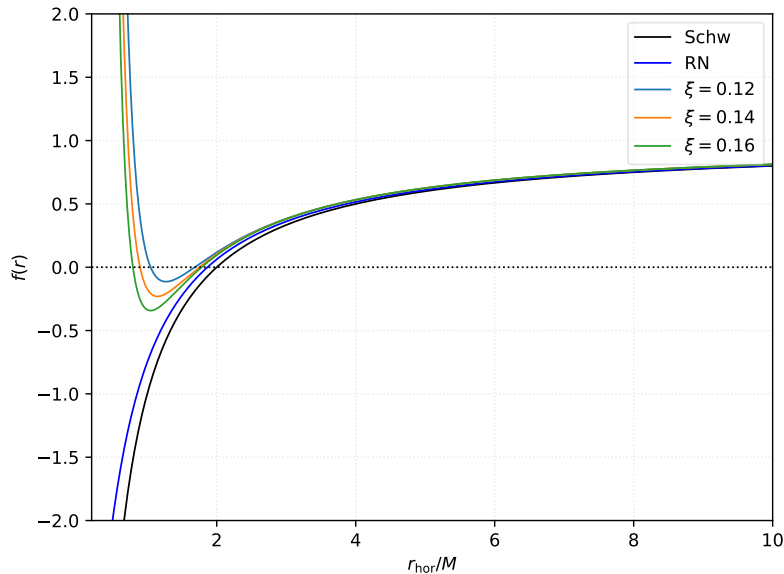


FIG. 1. Behavior of the metric function $f(r)$. Choosing a very small value for ξ makes the horizon to disappear. Here, we have chosen an arbitrary value of $Q/M = 0.50$ to enable comparison.

The metric function above follows all the Einstein field equations. This metric function for the limit $\xi \rightarrow 0$ gives the standard Reissner Nordström black hole.

$$f(r) = 1 - \frac{2M}{r} + \frac{Q^2}{r^2}. \quad (12)$$

while the exact behavior of $f(r)$ in the small ξ domain is,

$$f(r) = 1 - \frac{2M}{r} + \frac{Q^2}{r^2} + \xi \left(\frac{4Q^{3/2}\sqrt{2} \left(4 - 3\ln\left(\frac{8Q}{r}\right)\right)}{9r} \right) + \mathcal{O}(\xi^2). \quad (13)$$

The asymptotic behavior of this metric function is intriguing when the following form is considered:

$$f(r) = 1 - \frac{2M_{\text{ADM}}}{r} + \frac{Q^3}{9\xi^2 r^4} + \mathcal{O}\left(\frac{1}{r^6}\right), \quad (14)$$

where,

$$M_{\text{ADM}} = M + \frac{2\sqrt{2}}{3}\xi Q^{3/2} \ln\left(2\xi\sqrt{2Q}\right). \quad (15)$$

Fig. (1) depicts the behavior of the metric function, as compared to the Schwarzschild and Reissner-Nordstrom BHs. The plot of the lapse function $f(r)$ reveals important properties of the horizons for the magnetically charged black hole. The event horizons are identified where $f(r) = 0$, and the presence of multiple horizons suggests deviations from the simple Schwarzschild case. As the parameter ξ increases, the outer horizon shifts inwards. Compared to the RN and Schwarzschild solutions, the modified black hole exhibits a richer horizon structure, potentially affecting its stability and causal properties.

III. CALCULATION OF THE WEAK FIELD DEFLECTION ANGLE

Without loss of generality, we solely focus on the orbital equation, trajectory, and finally the deflection angle. We will study the deflection angle of particles in RN spacetime while treating the optical metric as the background space. We will compare our results with the Schw. like spacetime.

A. Jacobi metric and particle in Equatorial plane

Assume a static spherically symmetric line element (SSS metric):

$$ds^2 = -A(r) dt^2 + B(r) dr^2 + C(r) d\Omega^2, \quad (16)$$

its Jacobi metric is written as:

$$\begin{aligned} dl^2 &= g_{ij} dx^i dx^j, \\ &= (E_1^2 - m_1^2 A) \left(\frac{B}{A} dr^2 + \frac{C}{A} d\Omega^2 \right). \end{aligned} \quad (17)$$

where m_1 and E_1 represent the mass and energy of the particle. For the optical metric, we need $m_1 = 0$ and $E_1 = 1$. At infinity, the energy of the particle becomes,

$$E_1 = \frac{m_1}{\sqrt{1-v^2}}. \quad (18)$$

In the equatorial plane ($\theta = \frac{\pi}{2}$), jacobic metric reads as:

$$dl^2 = m_1^2 \left(\frac{1}{1-v^2} - A \right) \left(\frac{B}{A} dr^2 + \frac{C}{A} d\phi^2 \right). \quad (19)$$

The trajectory equation of a particle can be written as [96]:

$$\left(\frac{du}{d\phi} \right)^2 = \frac{C^4 u^4}{AB} \left\{ \frac{1}{b^2 v^2} - A \left(\frac{1-v^2}{b^2 v^2} - \frac{1}{C} \right) \right\}, \quad (20)$$

where u is defined as $u = \frac{1}{r}$ and b stands for the impact parameter. Putting $v=1$ gives the null geodesic equation as:

$$\left(\frac{du}{d\phi} \right)^2 = \frac{C^4 u^4}{AB} \left[\frac{1}{b^2} - \frac{A}{C} \right]. \quad (21)$$

For constant r , say $r = r_{co} = \gamma_{co}$, the Eq. (19) becomes,

$$dl^2 = m_1^2 \left(\frac{1}{(1-v^2)A(r_{co})} - 1 \right) C(r_{co}) d\phi^2. \quad (22)$$

The curvature has the following form [96]:

$$\mathcal{K}(\gamma_{co}) = \sqrt{g_{rr} \left(\Gamma_{\phi\phi}^r \right)^2} \left(\frac{d\phi}{dl} \right)^2 \Big|_{r=r_{co}}, \quad (23)$$

Taking $\mathcal{K}(\gamma_{co}) = 0$ gives,

$$C(r_{co}) \partial_r A(r_c) - A(r_{co}) \partial_r C(r_{co}) [1 - A(r_{co}) + v^2 A(r_{co})] = 0, \quad (24)$$

For light $v = 1$,

$$C(r_{co}) \partial_r A(r_c) - A(r_{co}) \partial_r C(r_{co}) = 0, \quad (25)$$

Putting $C(r) = r^2$ gives,

$$r_{co} \partial_r A(r_{co}) - 2A(r_{co}) = 0. \quad (26)$$

which is in agreement with the [97].

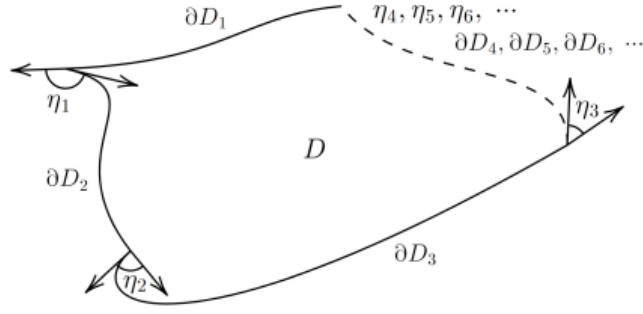


FIG. 2. Boundary of region D is defined as $\partial D = \cup_i \partial D_i$ while η_i denote the jump angles [99].

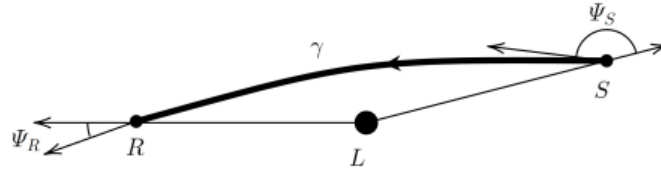


FIG. 3. L stands for the lens, S and R are the source and the observer of particles, respectively. γ represents the trajectory from S to R [99].

B. Gauss Bonnet Theorem and Lensing Geometry

GBT associates the intrinsic differential geometry of a surface with its topology. It deals with the geodesic triangles on the surfaces [98]. Consider D be a compact and connected region on a two-dimensional Riemannian manifold as depicted in the Fig (2). Boundary of D region is $\partial D_1, \partial D_2, \dots$ so GBT states that:

$$\int \int_D K dS + \sum_i \int_{\partial D_i} \kappa dl + \sum_i \eta_i = 2\pi \chi(D), \quad (27)$$

where K and dS denote the Gaussian curvature and area element of D , κ stands for the geodesic curvature, and dl represents the line element of ∂D and $\chi(D)$ denotes the Euler characteristic number of D . So, GBT states the relationship between geometric property of surfaces and their topological characteristics. By definition the deflection angle is,

$$\alpha \equiv \Psi_R - \Psi_S + \phi_{RS}, \quad (28)$$

S and R are the source and the receiver of particles, respectively. Fig. (3) represents all these entities in best way. Ψ_R and Ψ_S stands for the angles between the tangent of the γ and vectors drawn radially outward at S and R . When source and receiver are at infinite distance from the lens then $\Psi_S = \pi$ and $\Psi_R = 0$ the deflection angle is called as the infinite-distance deflection angle written as

$$\alpha = \phi_{RS} - \pi, \quad (29)$$

Deflection angle for the asymptotically non-flat spacetime is,

$$\alpha = \int \int_D K dS + \phi_{RS}. \quad (30)$$

while the curvature is written as [21],

$$K = \frac{1}{\sqrt{\det g}} \left(\frac{\partial}{\partial \phi} \left(\frac{\sqrt{\det g}}{g_{rr}} \Gamma_{rr}^\phi \right) - \frac{\partial}{\partial r} \left(\frac{\sqrt{\det g}}{g_{rr}} \Gamma_{r\phi}^\phi \right) \right). \quad (31)$$

From the optical metric, one gets:

$$g_{rr} = \frac{B}{A},$$

$$\begin{aligned} \det g &= \frac{BC}{A^2}, \\ \Gamma_{r\phi}^\phi &= \frac{1}{2} \left(\frac{C'}{C} - \frac{A'}{A} \right), \end{aligned} \quad (32)$$

Then by using Eq. (31),

$$\begin{aligned} \int K \sqrt{\det g} dr &= - \int \frac{d \left(\frac{\sqrt{\det g} \Gamma_{r\phi}^\phi}{g_{rr}} \right)}{dr} dr, \\ &= - \frac{\sqrt{\det g} \Gamma_{r\phi}^\phi}{g_{rr}}, \\ &= \frac{(CA' - C'A)}{2A\sqrt{BC}}. \end{aligned} \quad (33)$$

whereas,

$$\int K \sqrt{\det g} dr \Big|_{r=r_{co}} = 0. \quad (34)$$

and so Eq. (30) gets the following form:

$$\alpha = \int_{\phi_S}^{\phi_R} \int_{r_{co}}^{r(\phi)} K \sqrt{\det g} dr d\phi + \phi_{RS}. \quad (35)$$

where $r(\phi) = \frac{1}{u}$. In the upcoming section, we will study the application of GBT where the considered metric is the exact solution of the Einstein equation presented in Eq. (6).

C. Application of GBT

The asymptotic behavior of the metric function for the RN black hole is more intriguing when the following form of metric is considered [95],

$$\begin{aligned} A(r) &= 1 - \frac{2M_{\text{ADM}}}{r} + \frac{Q^3}{9\xi^2 r^4} + \mathcal{O}\left(\frac{1}{r^6}\right), \\ B(r) &= \frac{1}{A(r)}. \end{aligned} \quad (36)$$

Here, M_{ADM} (the ADM stands for Arnowitt-Deser-Misner) is the combined mass, namely the Schwarzschild mass M and the electromagnetic mass $M_e = \frac{2\sqrt{2}}{3}\xi Q^{3/2} \ln(2\xi\sqrt{2Q})$, where the absence of non-linear electrodynamics leads to the $M = M_e$ [95].

$$M_{\text{ADM}} = M + \frac{2\sqrt{2}}{3}\xi Q^{3/2} \ln(2\xi\sqrt{2Q}). \quad (37)$$

The orbit equation of a particle moving in the equatorial plane can be written as:

$$\left(\frac{du}{d\phi} \right)^2 = \frac{C^4 u^4}{AB} \left[\frac{1}{b^2 v^2} - A \left(\frac{1-v^2}{b^2 v^2} - \frac{1}{C} \right) \right],$$

for $v = 1$:

$$\left(\frac{du}{d\phi} \right)^2 = \frac{C^4 u^4}{AB} \left[\frac{1}{b^2} - \frac{A}{C} \right]. \quad (38)$$

by using the following equation, we evaluate the trajectory of the particle.

$$C(r_{co}) \partial_{r_{co}} A(r_{co}) - A(r_{co}) \partial_r C(r_{co}) = 0,$$

(39)

By using this equation, we got:

$$\begin{aligned}
 a &= \left(81M^2Q^3\xi^4 + \sqrt{-256Q^9\xi^6 + 6561M^4Q^6\xi^8} \right)^{\frac{1}{3}}, \\
 r_{\text{co}} &= \frac{3M}{4} + \frac{\sqrt{27M^2a\xi^2 + 16 \cdot 2^{\frac{1}{3}}Q^3\xi^2 + 2 \cdot 2^{\frac{2}{3}}a^2}}{4\sqrt{3a\xi}} + \left(\frac{1}{2} \frac{9M^2}{2} - \frac{4 \cdot 2^{\frac{1}{3}}Q^3}{3a} - \frac{a}{3 \cdot 2^{\frac{1}{3}}\xi^2} \right. \\
 &\quad \left. + \frac{27\sqrt{3a\xi}M^3}{2\sqrt{27aM^2\xi^2 + 16 \cdot 2^{\frac{1}{3}}Q^3\xi^2 + 2 \cdot 2^{\frac{2}{3}}a^2}} \right)^{\frac{1}{2}}.
 \end{aligned} \tag{40}$$

Now defining $A(r)$, $B(r)$ and $C(r)$,

$$\begin{aligned}
 A(r) &= 1 - \frac{2M_{\text{ADM}}}{r} + \frac{Q^3}{9\xi^2 r^4}, \\
 B(r) &= \frac{1}{A(r)}, \\
 C(r) &= r^2.
 \end{aligned} \tag{41}$$

The orbit equation deduced in this case is:

$$\left(\frac{du}{d\phi} \right)^2 = \frac{1}{b^2} - u^2 + 2M_{\text{ADM}}u^3 - \frac{Q^3u^6}{3\xi^2}. \tag{42}$$

solution of above equation found by the iterative method is:

$$u = \frac{\sin \phi}{b} + \frac{M_{\text{ADM}}(1 + \cos^2 \phi)}{b^2} - \frac{80Q^3 \sin \phi}{384b^5\xi^2} + \mathcal{O}\left(M_{\text{ADM}}^2, \xi^2, (Q^3)^2\right). \tag{43}$$

Gauss Theorema Egregium states that "the Gaussian curvature just depends on angles, distances, and their rates of change." Let $X : u \rightarrow \mathcal{R}^3$ is the patch then the Gaussian curvature adapts the following form:

$$\mathcal{K} = -\frac{1}{2}\sqrt{EG} \left(\frac{\partial}{\partial u} \left(\frac{G_u}{\sqrt{EG}} \right) + \frac{\partial}{\partial v} \left(\frac{E_v}{\sqrt{EG}} \right) \right). \tag{44}$$

where E ,G stands for the matrices defined as,

$$\begin{aligned}
 E &= h(Y_u, Y_u), \\
 G &= h(Y_\nu, Y_\nu). \quad \text{where } Y_{u,\nu} = \partial_{u,\nu}Y
 \end{aligned}$$

where the full details are given in [100] whereas Gauss Theorema Egregium is the consequence of Brioschis formula. Gauss curvature can also be determined by relating the Riemannian tensor's independent component with it, that is $\mathcal{K} = R_{1212}/\det(g)$. The curvature determined from the Eq. (31) is:

$$\begin{aligned}
 \mathcal{K} &= \frac{M_{\text{ADM}}(3M_{\text{ADM}} - 2r)}{r^4} + \frac{2Q^6}{27r^{10}\xi^4} - \frac{2Q^3(9M_{\text{ADM}} - 5r)}{9r^7\xi^2}, \\
 &= \frac{3M^2}{r^4} - \frac{2M}{r^3} + \frac{2Q^6}{27r^{10}\xi^4} - \frac{2MQ^3}{r^7\xi^2} + \frac{10Q^3}{9r^6\xi^2} - \frac{4\sqrt{2}Q^{9/2} \ln(2\sqrt{2}\sqrt{Q}\xi)}{3r^7\xi} + \frac{4\sqrt{2}MQ^{3/2}\xi \ln(2\sqrt{2}\sqrt{Q}\xi)}{r^4} - \\
 &\quad \frac{4\sqrt{2}Q^{3/2}\xi \ln(2\sqrt{2}\sqrt{Q}\xi)}{3r^3} + \frac{8Q^3\xi^2 \ln(2\sqrt{2}\sqrt{Q}\xi)^2}{3r^4}.
 \end{aligned} \tag{45}$$

Our prime concern is the asymptotic bending angle that is,

$$\alpha = \int \mathcal{K} \sqrt{\det(g_{\text{opt}})} dr d\phi,$$

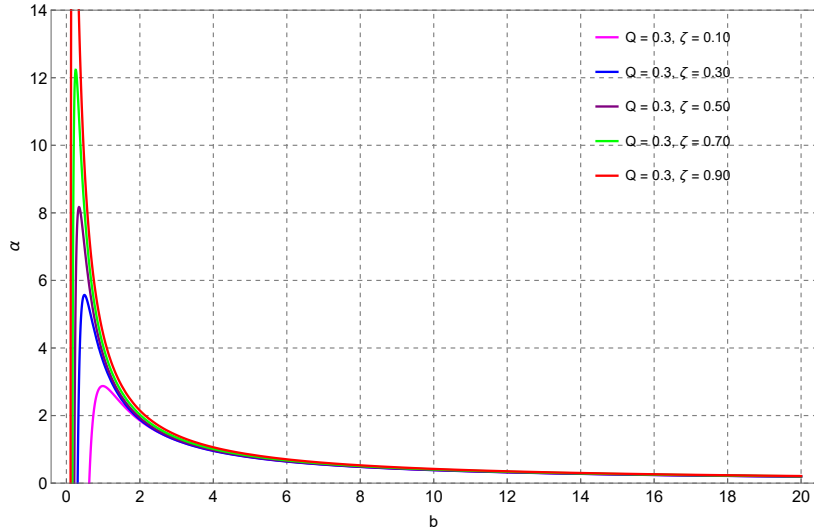


FIG. 4. We kept $M=1$, $Q=0.3$ for the deflection angle " α " Vs impact parameter " b "

$$\int \mathcal{K} \sqrt{\det g} dr d\phi = \int_0^\pi \int_{\frac{b}{\sin \phi}}^\infty \sqrt{\frac{r^2}{\left(1 - \frac{2M}{r} + \frac{Q^3}{9\xi^2 r^4}\right)^3}} \mathcal{K} dr d\phi, \quad (46)$$

So, the deflection angle corresponding to the interesting asymptotic behavior of the modified metric $A(r) = 1 - \frac{2M_{\text{ADM}}}{r} + \frac{Q^3}{9\xi^2 r^4}$ in Schwarzschild (asymptote) spacetime is:

$$\alpha = \frac{4M}{b} - \frac{5\pi Q^3}{48b^4 \xi^2} + \frac{\sqrt{2}M\pi Q^{3/2} \xi \ln(2\sqrt{2}\sqrt{Q}\xi)}{b^2} + \frac{64MQ^3 \xi^2 \ln(2\sqrt{2}\sqrt{Q}\xi)^2}{9b^3} + \frac{8\sqrt{2}Q^{3/2} \xi \ln(2\sqrt{2}\sqrt{Q}\xi)}{3b} + \frac{2\pi Q^3 \xi^2 \ln(2\sqrt{2}\sqrt{Q}\xi)^2}{3b^2} + \mathcal{O}(M^2, \xi^2, (Q^3)^2). \quad (47)$$

This deflection angle expression encapsulates both the standard Schwarzschild term, $\frac{4M}{b}$, and additional corrections arising from the modified metric $A(r)$ where the extra terms, featuring both power-law and logarithmic dependences on the impact parameter b , reflect non-trivial modifications due to the charge-like parameter Q and the coupling ξ . These corrections, which become more pronounced for smaller b , hint at richer underlying physics such as non-linear electrodynamics or higher-curvature effects and suggest observable deviations in gravitational lensing, with the expansion being perturbative in M , ξ , and Q^3 . For Schwarzschild spacetime, the deflection angle can be obtained from the above expression by taking $Q \rightarrow 0$ and $\xi \rightarrow 0$, that is, $\frac{4M}{b}$.

A graphical depiction of the deflection angle for different values of ξ is shown in Fig. 4. This plot illustrates the gravitational deflection angle α as a function of the impact parameter b for a magnetically charged black holes in nonlinear electrodynamics with mass $M = 1$ and charge $Q = 0.3$, analyzed under different values of the parameter ζ . The results indicate that for small impact parameters, the deflection angle exhibits a sharp peak, with the magnitude of bending increasing as ζ grows. This suggests that ζ enhances the gravitational lensing effect, potentially modifying the spacetime geometry and amplifying light bending. As b increases, the deflection angle decreases and converges toward zero, consistent with weak-field gravitational lensing expectations. These deviations from standard Reissner-Nordström behavior could have observational implications for black hole lensing and shadow analysis, providing potential tests for modified gravity models.

When light just passes closest to the source then the post-Newtonian (PPN) formalism equation for light deflection is written as [101],

$$\alpha = 175'' \left(\frac{1 + \gamma}{2} \right). \quad (48)$$

where γ is the PPN deflection parameter [102]. By equating Eq. (47) and Eq. (48), the constraint on the RN scale can be determined easily which comes out to be:

$$0 < \xi < 4.7 \times 10^{-2}. \quad (49)$$

The tight bound on ξ has significant implications. Many alternative theories of gravity predict modifications to the standard gravitational potential, and these modifications often manifest in observable quantities such as the deflection of light. This result implies that any extra contributions to the gravitational potential, parameterized by ξ , must be very small to remain consistent with the observed light deflection. In effect, the observational success of GR in explaining light bending forces the RN-scale modifications (or analogous corrections) to lie within a narrow range. Any theory predicting a larger value of ξ would lead to a deflection angle in conflict with high-precision solar system measurements. Thus, this relation acts as an important filter for theoretical models, ruling out those that cannot accommodate the smallness of ξ .

IV. CALCULATION OF THE STRONG DEFLECTION OF ANGLE PHOTONS

Investigating the effects of black holes on the photons in the strong-field region, we employ the methodology of Tsukamoto in Ref. [92]. The strong deflection angle is derived using the orbit equation expressed as,

$$\left(\frac{dr}{d\phi}\right)^2 = \frac{\mathcal{R}(r)r^2}{B(r)}, \quad (50)$$

where

$$\mathcal{R}(r) = \frac{A(r_0)r^2}{A(r)r_0^2} - 1. \quad (51)$$

We define $A(r)$ as the metric function defined by Eq. (14) and (15), while $A(r_0)$ is the metric function evaluated at distance r_0 . The solution of Eq. (50) yields the strong deflection angle $\alpha(r_0)$ as shown in Ref. [91, 92]

$$\begin{aligned} \alpha(r_0) &= I(r_0) - \pi \\ &= 2 \int_{r_0}^{\infty} \frac{dr}{\sqrt{\frac{\mathcal{R}(r)C(r)}{B(r)}}} - \pi. \end{aligned} \quad (52)$$

In order to evaluate the integral in Eq. (52), we employ series expansion over $r = r_0$. This yields a regular integral κ_R and a diverging integral κ_D . Using the new variable, z , defined as,

$$z \equiv 1 - \frac{r_0}{r}, \quad (53)$$

$I(r_0)$ is expressed as,

$$I(r_0) = \int_0^1 \kappa(z, r_0) dz = \int_0^1 [\kappa_D(z, r_0) + \kappa_R(z, r_0)] dz, \quad (54)$$

where $\kappa(z, r_0)$ is expressed as the sum of the diverging integral, κ_D , and regular integral, κ_R . The details of the expansion of Eq. (52) was shown in Refs. [91, 92]. As a result the strong deflection angle is expressed as,

$$\hat{\alpha}_{\text{str}} = -\bar{a} \log\left(\frac{b_0}{b_{\text{crit}}} - 1\right) + \bar{b} + O\left(\frac{b_0}{b_c} - 1\right) \log\left(\frac{b_0}{b_c} - 1\right), \quad (55)$$

where \bar{a} and \bar{b} are coefficients of deflection angle and b_0 and b_{crit} are the impact parameter evaluated at the closest approach, r_0 , and critical impact parameter, respectively. The first term in Eq. (55) is the result of the diverging integral and the second term is the result of the regular integral. The coefficients \bar{a} and \bar{b} are expressed as [92],

$$\bar{a} = \sqrt{\frac{2B(r_{\text{ps}})A(r_{\text{ps}})}{2A(r_{\text{ps}}) - A''(r_{\text{ps}})r_{\text{ps}}^2}}, \quad (56)$$

and

$$\bar{b} = \bar{a} \log\left[r_{\text{ps}} \left(\frac{2}{r_{\text{ps}}^2} - \frac{A''(r_{\text{ps}})}{A(r_{\text{ps}})}\right)\right] + I_R(r_{\text{ps}}) - \pi, \quad (57)$$

where $A(r_{\text{ps}})$ is metric function evaluated at the photon sphere, and I_R is the regular integral evaluated from 0 to 1. The double prime in Eq. (56) and Eq. (57) correspond to the second derivative with respect to r evaluated on r_{ps} .

The metric functions presented above are derived through a series expansion. Unlike the Reissner Nordström (RN) black hole metric, where the charge contributes independently via the term Q/r^2 , in this case, the charge contribution is coupled with the mass, M_{ADM} , and additional parameter ξ , as shown in Eq. (15). Additionally, the contribution of the third term in Eq. (14) is negligible because $Q \ll M$, and its impact is proportional to the fourth power of the radial position. However, the effect of the charge on the strong deflection angle (SDA) can still be analyzed by considering only the first two terms of the metric function $A(r)$.

Now, we have an approximate expression of,

$$A(r) = 1 - \frac{2M_{ADM}}{r} \quad (58)$$

and

$$B(r) = \frac{1}{A(r)}. \quad (59)$$

The above metric now resembles a Schwarzschild metric. As one of the important properties of the black hole metric, we have to calculate the photon sphere, using the equation in Eq. (26), we approximate it to be,

$$r_{ph} = 3M_{ADM}. \quad (60)$$

Evaluating the coefficients \bar{a} and the argument of the logarithmic term in \bar{b} using the equations (56) and (57), respectively, yields,

$$\begin{aligned} \bar{a} &= 1 \\ \bar{b} &= \log[6] + I_R(r_{ps}) - \pi. \end{aligned} \quad (61)$$

The coefficients of \bar{a} and \bar{b} are consistent with the strong Schwarzschild deflection coefficient, as shown in Ref. [91]. It suggests that the strong lensing of the black hole metric is analogous to the Schwarzschild black hole.

The regular integral I_R is defined as,

$$I_R(r_0) \equiv \int_0^1 f_R(z, r_0) - f_D(z, r_0) dz, \quad (62)$$

where the $f_R(z, r_0)$ was generated from the expansion of the trajectory in Eq. (50), which gives us

$$f_R(z, r_0) = \frac{2r_0}{\sqrt{G(z, r_0)}}, \quad (63)$$

where $G(z, r_0) = RCA(1-z)^4$. Notice that C and A are the metric functions for which the position ρ is expressed in terms of z and r_0 , while R is shown in Eq. (51). The generated expression from Eq. (63) is,

$$f_R(z, r_{ps}) = \frac{2r_{ps}}{\sqrt{\sum_{m=2}^m c_m(r_{ps})z^m}}, \quad (64)$$

when we evaluate $r_0 = r_{ps}$. On the other hand the $f_D(z, r_{ps})$ is expressed as,

$$f_D(z, r_{ps}) = \frac{2r_{ps}}{\sqrt{c_2 z^2}}, \quad (65)$$

where the c 's are coefficients of the new variable z . Evaluating the integral $I_R(r_0)$ as $r_0 \rightarrow r_{ps}$ yields,

$$I_R(r_{ps}) = \ln \left(\frac{144}{(1 + \sqrt{3})^{1/4}} \right). \quad (66)$$

The strong deflection is now expressed as,

$$\hat{\alpha}_{str} = -\log \left(\frac{b_0}{b_{crit}} - 1 \right) + \log \left[\frac{144}{(1 + \sqrt{3})^{1/4}} \right] - \pi + O \left(\frac{b_0}{b_c} - 1 \right) \log \left(\frac{b_0}{b_c} - 1 \right). \quad (67)$$

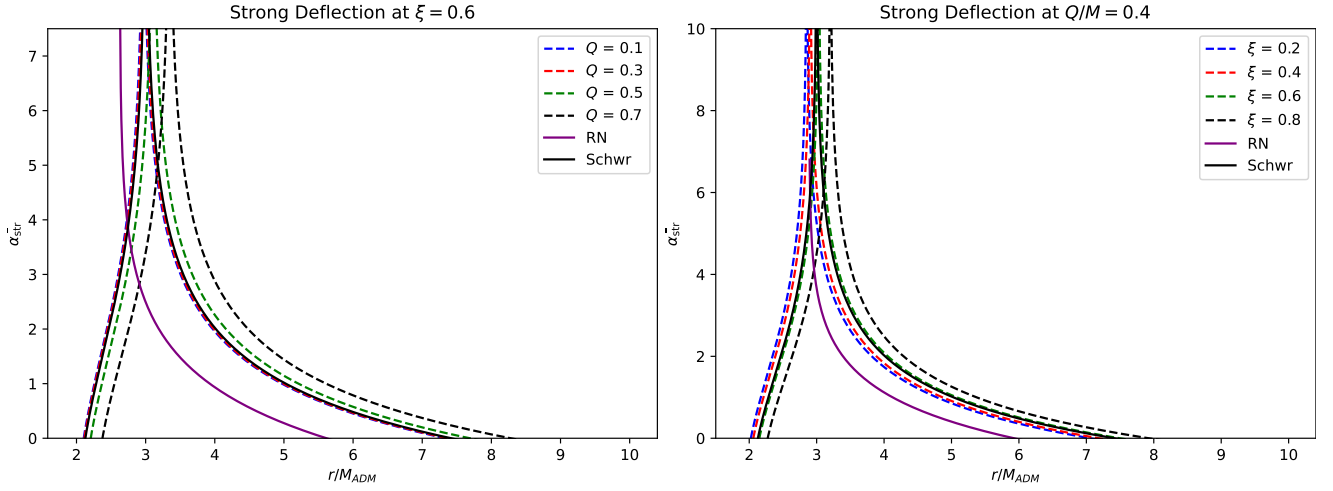


FIG. 5. Strong deflection angle with varying parameters Q and ξ . In the left figure we use the $\xi = 0.6$, while on the right hand side we use $Q/M = 0.4$

To calculate the impact parameter we utilize equation (71) and note that $r \rightarrow r_0$ this will generate the impact parameter for the closest approach,

$$b_0^2 = \frac{r_0^3}{r_0 - 2M_{ADM}}, \quad (68)$$

when the $r_0 \rightarrow 3M_{ADM}$ it yields the critical impact parameter, $b_{crit} = 3\sqrt{3}M_{ADM}$.

Figure 5 illustrates the influence of the black hole parameters ξ and Q within the strong-field regime. The left panel demonstrates that, at specific values of ξ , the charge Q induces a noticeable deviation from the predictions of the Schwarzschild and RN black hole. This observation indicates that the charge Q exerts a significant influence on the photon sphere, a region where the deflection angle diverges. Moreover, the effects of variations in the parameter ξ are found to align consistently with changes in Q , highlighting the coupled interplay between these two parameters.

V. SHADOW CAST

In studying the shadow of any static and spherically symmetric black hole, methods are widely known [103, 104] and used in many studies present in the literature. We follow such methods in this work and summarize the most important part of the expressions needed to study the black hole shadow. One usually begins with the Lagrangian or Hamiltonian for light rays, then obtains the equations of motion, and the orbit equation. From the orbit equation, the photon sphere can be solved by taking the derivative of the function,

$$h(r) = \frac{C(r)}{A(r)}, \quad (69)$$

with respect to r , and setting to zero. It results to the expression:

$$h'(r) = C'(r)A(r) - C(r)A'(r) = 0. \quad (70)$$

Depending on the metric functions' complexity, we may or may not obtain some analytical solution to r_{co} . The derivation for the shadow becomes simple if there is an analytical solution for r_{co} . From Eqs. (14-15), it is not possible to obtain an analytical solution. To know the behavior of the photon sphere under the influence of the parameter ξ , we rely on numerical considerations shown in Fig. 6. We found that ξ causes a smaller photon sphere radius as compared to the RN case. The radius is even smaller, as ξ decreases.

The most important quantity in the formation of the shadow is the critical impact parameter of light, defined by,

$$b_{crit}^2 = \frac{C(r_{co})}{A(r_{co})}, \quad (71)$$

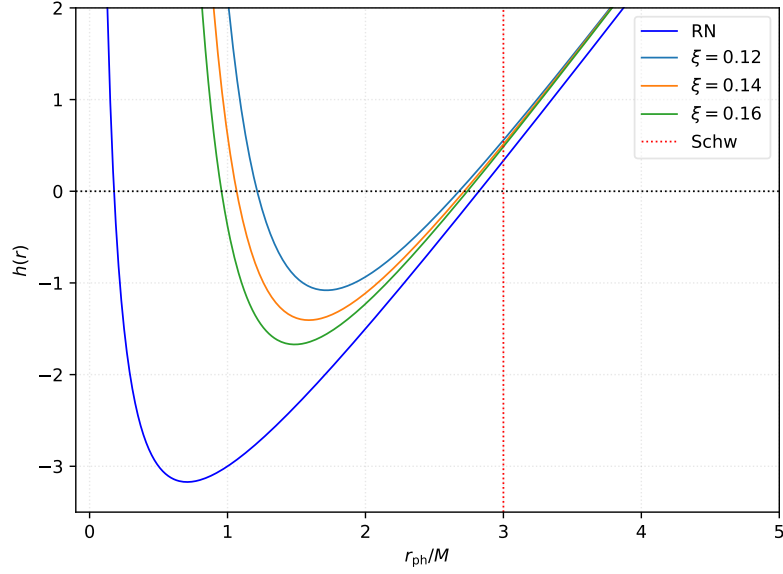


FIG. 6. Behavior of the photon sphere. Here, we have chosen an arbitrary value of $Q/M = 0.50$ to enable comparison. The vertical dotted line is the photon sphere radius for the Schwarzschild case.

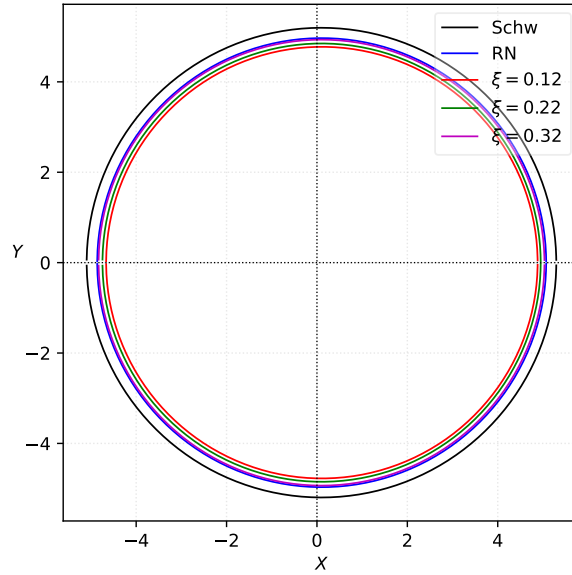


FIG. 7. Behavior of the shadow cast. Here, we have chosen an arbitrary value of $Q/M = 0.50$ to enable comparison. The plot shown is in terms of the Cartesian system.

and the analytic expression of the shadow can then be calculated using:

$$R_{\text{sh}} = b_{\text{crit}} \sqrt{A(r_{\text{obs}})}. \quad (72)$$

Again, while the resulting expression can be quite complicated to study it analytically, we used numerical approach in order to visualize the shadow cast. This is shown in Fig. 7. First, we observe that while the deviation from the RN case is quite noticeable in r_{co} for $\xi = 0.12$ to $\xi = 0.16$, the deviation in the shadow cast is not too noticeable. Hence, to show strong deviation, the values of ξ are increased on the plot. In essence, we can tell that decreasing the photon sphere results in a decrease in the shadow radius. Furthermore, the shadow radius also decreases as we decrease ξ .

VI. CONCLUSION

In this work, we have investigated the gravitational lensing characteristics and shadow formation of a magnetically charged black hole within the framework of nonlinear electrodynamics. Using a geometric approach based on the Gauss-Bonnet theorem, we derived the trajectory equation, the Gaussian curvature, and an analytical expression for the weak-field deflection angle of light propagating in the equatorial plane. Our analysis shows that the standard Schwarzschild deflection term, $4M/b$, is augmented by additional corrections that depend on both the magnetic charge Q and the nonlinear coupling parameter ξ . These extra contributions, which appear as power-law and logarithmic terms, highlight the nontrivial influence of nonlinear electromagnetic effects on the spacetime geometry and underscore modifications in the Reissner-Nordström (RN) metric relative to the Schwarzschild case.

In the strong-field regime, we further analyzed the behavior of light rays near the photon sphere by employing the strong deflection limit formalism. In this limit, the deflection angle exhibits the familiar logarithmic divergence as the impact parameter approaches its critical value. The derived strong deflection coefficients, \bar{a} and \bar{b} , reveal that the presence of the nonlinear electrodynamic (NED) charge enhances the bending of light compared to the standard RN case. This enhancement, arising from the coupled interplay between Q and ξ , not only affects the near-horizon geodesics but also has significant implications for the structure of the photon sphere and the corresponding black hole shadow.

Our numerical analysis indicates that increasing the coupling parameter ξ or the charge Q leads to a reduction in the radius of the photon sphere, thereby producing a smaller shadow. Such behavior distinguishes nonlinear electrodynamic black holes from their classical counterparts and offers a potential observational signature that could be tested in future high-resolution imaging experiments. Moreover, the tight constraints imposed on ξ by solar system light-bending observations ensure that any deviations from classical predictions remain within acceptable observational limits, thereby reinforcing the consistency of our approach.

The results presented here provide some hints about the key importance of the modifications induced by nonlinear electrodynamics on both the gravitational lensing and shadow characteristics of black holes. They demonstrate the potential of precision lensing and shadow observations to probe deviations from standard general relativity and to test the viability of alternative theories of gravity in extreme astrophysical environments.

ACKNOWLEDGMENTS

A. Ö. and R. P. would like to acknowledge networking support of the COST Action (CA) 18108 - Quantum gravity phenomenology in the multi-messenger approach, CA 22113 - Fundamental challenges in theoretical physics (Theory and Challenges), CA 21106 - COSMIC WISPerS in the Dark Universe: Theory, astrophysics and experiments (CosmicWISPerS), CA 21136 - Addressing observational tensions in cosmology with systematics and fundamental physics (CosmoVerse), and CA 23130 - Bridging high and low energies in search of quantum gravity (BridgeQG). We also thank TUBITAK and SCOAP3 for their support.

-
- [1] M. Kline, *Mathematical Thought from Ancient to Modern Times*. Oxford: Oxford University Press, 1972.
 - [2] S. Bandyopadhyay, B. Dacorogna, V. Matveev, and M. Troyanov, "Bernhard riemann 1861 revisited: existence of flat coordinates for an arbitrary bilinear form," *Mathematische Zeitschrift*, vol. 305, no. 12, 2023.
 - [3] A. Einstein, "The foundation of the general theory of relativity.," *Annalen Phys.*, vol. 49, no. 7, pp. 769–822, 1916.
 - [4] C. W. Misner, K. S. Thorne, and J. A. Wheeler, *Gravitation*. San Francisco: Freeman W. H. and Company, 1973.
 - [5] W. Rindler, *Essential Relativity: Special, General, and Cosmological*. Springer Verlag, 2nd ed., 1977.
 - [6] F. W. Dyson, A. S. Eddington, and C. Davidson, "A determination of the deflection of light by the sun's gravitational field, from observations made at the total eclipse of may 29, 1919," *Philosophical Transactions of the Royal Society of London. Series A, Containing Papers of a Mathematical or Physical Character*, vol. 220, pp. 291–333, 1920.
 - [7] N. Tsukamoto, T. Harada, and K. Yajima, "Can we distinguish between black holes and wormholes by their Einstein ring systems?," *Phys. Rev. D*, vol. 86, p. 104062, 2012.
 - [8] C. R. Keeton, C. S. Kochanek, and E. E. Falco, "The Optical properties of gravitational lens galaxies as a probe of galaxy structure and evolution," *Astrophys. J.*, vol. 509, pp. 561–578, 1998.
 - [9] K. S. Virbhadra and G. F. R. Ellis, "Schwarzschild black hole lensing," *Phys. Rev. D*, vol. 62, p. 084003, 2000.
 - [10] H. Khodabakhshi and R. B. Mann, "Gravitational Lensing by Black Holes in Einstein Quartic Gravity," *Phys. Rev. D*, vol. 103, no. 2, p. 024017, 2021.
 - [11] K. S. Virbhadra and C. R. Keeton, "Time delay and magnification centroid due to gravitational lensing by black holes and naked singularities," *Phys. Rev. D*, vol. 77, p. 124014, 2008.
 - [12] L.-W. Chen, B.-J. Cai, C. M. Ko, B.-A. Li, C. Shen, and J. Xu, "Higher-order effects on the incompressibility of isospin asymmetric nuclear matter," *Phys. Rev. C*, vol. 80, p. 014322, Jul 2009.

- [13] M. Sharif and Z. Yousof, "Radiating cylindrical gravitational collapse with structure scalars in $f(R)$ gravity," *Astrophys. Space Sci.*, vol. 357, no. 1, p. 49, 2015.
- [14] W.-G. Cao and Y. Xie, "Weak deflection gravitational lensing for photons coupled to Weyl tensor in a Schwarzschild black hole," *Eur. Phys. J. C*, vol. 78, no. 3, p. 191, 2018.
- [15] G. S. Bisnovatyi-Kogan and O. Y. Tsupko, "Gravitational lensing in presence of plasma: Strong lens systems, black hole lensing and shadow," *Universe*, vol. 3, no. 3, 2017.
- [16] G. S. Bisnovatyi-Kogan and O. Y. Tsupko, "Gravitational lensing in a non-uniform plasma," *Mon. Not. Roy. Astron. Soc.*, vol. 404, pp. 1790–1800, 2010.
- [17] S. Refsdal, "On the possibility of determining Hubble's parameter and the masses of galaxies from the gravitational lens effect," *Mon. Not. Roy. Astron. Soc.*, vol. 128, p. 307, 1964.
- [18] M. Bartelmann and P. Schneider, "Weak gravitational lensing," *Phys. Rept.*, vol. 340, pp. 291–472, 2001.
- [19] P. Schneider, J. Ehlers, and E. E. Falco, *Gravitational lenses as astrophysical tools*. Springer, 1992.
- [20] C. Bloomer, "Optical Geometry of the Kerr Space-time," 11 2011.
- [21] M. C. Werner, "Gravitational lensing in the Kerr-Randers optical geometry," *Gen. Rel. Grav.*, vol. 44, pp. 3047–3057, 2012.
- [22] S. I. Godunov, A. N. Rozanov, M. I. Vysotsky, and E. V. Zhemchugov, "Extending the Higgs sector: an extra singlet," *Eur. Phys. J. C*, vol. 76, p. 1, 2016.
- [23] A. Ishihara, Y. Suzuki, T. Ono, T. Kitamura, and H. Asada, "Gravitational bending angle of light for finite distance and the Gauss-Bonnet theorem," *Phys. Rev. D*, vol. 94, no. 8, p. 084015, 2016.
- [24] A. Ishihara, Y. Suzuki, T. Ono, and H. Asada, "Finite-distance corrections to the gravitational bending angle of light in the strong deflection limit," *Phys. Rev. D*, vol. 95, no. 4, p. 044017, 2017.
- [25] K. Jusufi, M. C. Werner, A. Banerjee, and A. Övgün, "Light Deflection by a Rotating Global Monopole Spacetime," *Phys. Rev. D*, vol. 95, no. 10, p. 104012, 2017.
- [26] I. Sakalli and A. Övgün, "Hawking Radiation and Deflection of Light from Rindler Modified Schwarzschild Black Hole," *EPL*, vol. 118, no. 6, p. 60006, 2017.
- [27] P. Goulart, "Phantom wormholes in Einstein–Maxwell-dilaton theory," *Class. Quant. Grav.*, vol. 35, no. 2, p. 025012, 2018.
- [28] T. Ono, A. Ishihara, and H. Asada, "Gravitomagnetic bending angle of light with finite-distance corrections in stationary axisymmetric spacetimes," *Phys. Rev. D*, vol. 96, no. 10, p. 104037, 2017.
- [29] R. Fleischer, D. G. Espinosa, R. Jaarsma, and G. Tetlalmatzi-Xolocotzi, "CP Violation in Leptonic Rare B_s^0 Decays as a Probe of New Physics," *Eur. Phys. J. C*, vol. 78, no. 1, p. 1, 2018.
- [30] H. Arakida, "A note on the definitions of the relativistic perihelion advance," *General Relativity and Gravitation*, vol. 50, p. 1, 2018.
- [31] T. Ono, A. Ishihara, and H. Asada, "Deflection angle of light for an observer and source at finite distance from a rotating wormhole," *Phys. Rev. D*, vol. 98, no. 4, p. 044047, 2018.
- [32] K. Jusufi, A. Övgün, J. Saavedra, Y. Vásquez, and P. A. González, "Deflection of light by rotating regular black holes using the Gauss-Bonnet theorem," *Phys. Rev. D*, vol. 97, no. 12, p. 124024, 2018.
- [33] A. Övgün, "Light deflection by Damour-Solodukhin wormholes and Gauss-Bonnet theorem," *Phys. Rev. D*, vol. 98, no. 4, p. 044033, 2018.
- [34] A. Övgün, K. Jusufi, and I. Sakalli, "Exact traversable wormhole solution in bumblebee gravity," *Phys. Rev. D*, vol. 99, no. 2, p. 024042, 2019.
- [35] A. Övgün, "Weak field deflection angle by regular black holes with cosmic strings using the Gauss-Bonnet theorem," *Phys. Rev. D*, vol. 99, no. 10, p. 104075, 2019.
- [36] W. Javed, J. Abbas, and A. Övgün, "Deflection angle of photon from magnetized black hole and effect of nonlinear electrodynamics," *Eur. Phys. J. C*, vol. 79, no. 8, p. 694, 2019.
- [37] W. Javed, R. Babar, and A. Övgün, "Effect of the dilaton field and plasma medium on deflection angle by black holes in Einstein-Maxwell-dilaton-axion theory," *Phys. Rev. D*, vol. 100, no. 10, p. 104032, 2019.
- [38] K. de Leon and I. Vega, "Weak gravitational deflection by two-power-law densities using the Gauss-Bonnet theorem," *Phys. Rev. D*, vol. 99, no. 12, p. 124007, 2019.
- [39] R. Kumar, S. G. Ghosh, and A. Wang, "Shadow cast and deflection of light by charged rotating regular black holes," *Phys. Rev. D*, vol. 100, no. 12, p. 124024, 2019.
- [40] W. Javed, R. Babar, and A. Övgün, "The effect of the Brane-Dicke coupling parameter on weak gravitational lensing by wormholes and naked singularities," *Phys. Rev. D*, vol. 99, no. 8, p. 084012, 2019.
- [41] W. Javed, M. Aqib, and A. Övgün, "Effect of the magnetic charge on weak deflection angle and greybody bound of the black hole in Einstein-Gauss-Bonnet gravity," *Phys. Lett. B*, vol. 829, p. 137114, 2022.
- [42] G. Mustafa, A. Ditta, F. Javed, F. Atamurotov, I. Hussain, and B. Ahmedov, "Probing a black hole in Starobinsky-Bel-Robinson gravity with thermodynamical analysis, effective force and gravitational weak lensing," *Chin. J. Phys.*, vol. 90, pp. 494–508, 2024.
- [43] K. Gao and L.-H. Liu, "Microlensing and event rate of static spherically symmetric wormhole," *Phys. Lett. B*, vol. 858, p. 139019, 2024.
- [44] K. Gao, L.-H. Liu, and M. Zhu, "Microlensing effects of wormholes associated to blackhole spacetimes," *Phys. Dark Univ.*, vol. 41, p. 101254, 2023.
- [45] C.-K. Qiao and M. Zhou, "Gravitational lensing of Schwarzschild and charged black holes immersed in perfect fluid dark matter halo," *JCAP*, vol. 12, p. 005, 2023.
- [46] Y. Huang, B. Sun, and Z. Cao, "Extending Gibbons-Werner method to bound orbits of massive particles," *Phys. Rev. D*, vol. 107, no. 10, p. 104046, 2023.

- [47] W. Javed, M. Atique, R. C. Pantig, and A. Övgün, "Weak Deflection Angle, Hawking Radiation and Greybody Bound of Reissner–Nordström Black Hole Corrected by Bounce Parameter," *Symmetry*, vol. 15, no. 1, p. 148, 2023.
- [48] W. Javed, M. Atique, R. C. Pantig, and A. Övgün, "Weak lensing, Hawking radiation and greybody factor bound by a charged black holes with non-linear electrodynamics corrections," *Int. J. Geom. Meth. Mod. Phys.*, vol. 20, no. 03, p. 2350040, 2023.
- [49] W. Rindler and M. Ishak, "Contribution of the cosmological constant to the relativistic bending of light revisited," *Phys. Rev. D*, vol. 76, p. 043006, 2007.
- [50] M. Park, "Rigorous Approach to the Gravitational Lensing," *Phys. Rev. D*, vol. 78, p. 023014, 2008.
- [51] M. Sereno, "The role of Lambda in the cosmological lens equation," *Phys. Rev. Lett.*, vol. 102, p. 021301, 2009.
- [52] F. Simpson, J. A. Peacock, and A. F. Heavens, "On lensing by a cosmological constant," *Mon. Not. Roy. Astron. Soc.*, vol. 402, p. 2009, 2010.
- [53] Z. Li and T. Zhou, "Kerr black hole surrounded by a cloud of strings and its weak gravitational lensing in Rastall gravity," *Phys. Rev. D*, vol. 104, no. 10, p. 104044, 2021.
- [54] G. Aad *et al.*, "Search for flavour-changing neutral-current couplings between the top quark and the Higgs boson in multi-lepton final states in 13 TeV pp collisions with the ATLAS detector," *Eur. Phys. J. C*, vol. 84, no. 7, p. 757, 2024.
- [55] Z. Li and A. Övgün, "Finite-distance gravitational deflection of massive particles by a Kerr-like black hole in the bumblebee gravity model," *Phys. Rev. D*, vol. 101, no. 2, p. 024040, 2020.
- [56] H. Arakida, "Light deflection and Gauss–Bonnet theorem: definition of total deflection angle and its applications," *Gen. Rel. Grav.*, vol. 50, no. 5, p. 48, 2018.
- [57] K. Takizawa, T. Ono, and H. Asada, "Gravitational deflection angle of light: Definition by an observer and its application to an asymptotically nonflat spacetime," *Phys. Rev. D*, vol. 101, no. 10, p. 104032, 2020.
- [58] J. P. Luminet, "Image of a spherical black hole with thin accretion disk," *Astron. Astrophys.*, vol. 75, pp. 228–235, 1979.
- [59] K. Akiyama *et al.*, "First M87 Event Horizon Telescope Results. I. The Shadow of the Supermassive Black Hole," *Astrophys. J. Lett.*, vol. 875, p. L1, 2019.
- [60] K. Akiyama *et al.*, "First M87 Event Horizon Telescope Results. IV. Imaging the Central Supermassive Black Hole," *Astrophys. J. Lett.*, vol. 875, no. 1, p. L4, 2019.
- [61] K. Akiyama *et al.*, "First M87 Event Horizon Telescope Results. VI. The Shadow and Mass of the Central Black Hole," *Astrophys. J. Lett.*, vol. 875, no. 1, p. L6, 2019.
- [62] K. Akiyama *et al.*, "First Sagittarius A* Event Horizon Telescope Results. I. The Shadow of the Supermassive Black Hole in the Center of the Milky Way," *Astrophys. J. Lett.*, vol. 930, no. 2, p. L12, 2022.
- [63] K. Akiyama *et al.*, "First Sagittarius A* Event Horizon Telescope Results. III. Imaging of the Galactic Center Supermassive Black Hole," *Astrophys. J. Lett.*, vol. 930, no. 2, p. L14, 2022.
- [64] K. Akiyama *et al.*, "First Sagittarius A* Event Horizon Telescope Results. VI. Testing the Black Hole Metric," *Astrophys. J. Lett.*, vol. 930, no. 2, p. L17, 2022.
- [65] Z. Yan, "Employing shadow radius to constrain extra dimensions in black string space-time with dark matter halo," 12 2024.
- [66] X. Yang, "Observational appearance of the spherically symmetric black hole in PFDM," *Phys. Dark Univ.*, vol. 44, p. 101467, 2024.
- [67] Y. Yang, D. Liu, A. Övgün, G. Lambiase, and Z.-W. Long, "Black hole surrounded by the pseudo-isothermal dark matter halo," *Eur. Phys. J. C*, vol. 84, no. 1, p. 63, 2024.
- [68] L. Chakhchi, H. El Moumni, and K. Masmarr, "Signatures of the accelerating black holes with a cosmological constant from the Sgr A* and M87* shadow prospects," *Phys. Dark Univ.*, vol. 44, p. 101501, 2024.
- [69] K. Jafarzade, B. Eslam Panah, and M. E. Rodrigues, "Thermodynamics and optical properties of phantom AdS black holes in massive gravity," *Class. Quant. Grav.*, vol. 41, no. 6, p. 065007, 2024.
- [70] A. Övgün, L. J. F. Sese, and R. C. Pantig, "Constraints via the Event Horizon Telescope for Black Hole Solutions with Dark Matter under the Generalized Uncertainty Principle Minimal Length Scale Effect," *Annalen Phys.*, vol. 2023, p. 2300390, 9 2023.
- [71] R. C. Pantig, "Apparent and emergent dark matter around a Schwarzschild black hole," *Phys. Dark Univ.*, vol. 45, p. 101550, 2024.
- [72] K. Nozari, S. Saghafi, and M. Hassani, "Accretion onto a charged black hole in consistent 4D Einstein-Gauss-Bonnet gravity," *JHEAp*, vol. 45, pp. 214–230, 2025.
- [73] T.-T. Sui, Z.-L. Wang, and W.-D. Guo, "The effect of scalar hair on the charged black hole with the images from accretions disk," *Eur. Phys. J. C*, vol. 84, no. 4, p. 441, 2024.
- [74] S. Zare, L. M. Nieto, X.-H. Feng, S.-H. Dong, and H. Hassanabadi, "Shadows, rings and optical appearance of a magnetically charged regular black hole illuminated by various accretion disks," *JCAP*, vol. 08, p. 041, 2024.
- [75] A. A. Araújo Filho, "Static limit analysis of a nonlinear electromagnetic generalization of the Kerr-Newman black hole," 10 2024.
- [76] A. A. Araújo Filho, "Remarks on a nonlinear electromagnetic extension in AdS Reissner-Nordström spacetime," 10 2024.
- [77] A. Uniyal, S. Chakrabarti, R. C. Pantig, and A. Övgün, "Nonlinearly charged black holes: Shadow and thin-accretion disk," *New Astron.*, vol. 111, p. 102249, 2024.
- [78] R. Kumar Walia, "Exploring nonlinear electrodynamics theories: Shadows of regular black holes and horizonless ultracompact objects," *Phys. Rev. D*, vol. 110, no. 6, p. 064058, 2024.
- [79] A. Uniyal, S. Chakrabarti, M. Fathi, and A. Övgün, "Observational signatures: Shadow cast by the effective metric of photons for black holes with rational non-linear electrodynamics," *Annals Phys.*, vol. 462, p. 169614, 2024.
- [80] G. Lambiase, R. C. Pantig, and A. Övgün, "Weak field deflection angle and analytical parameter estimation of the Lorentz-violating Bumblebee parameter through the black hole shadow using EHT data," *EPL*, vol. 148, no. 4, p. 49001, 2024.

- [81] R. C. Pantig, S. Kala, A. Övgün, and N. J. L. S. Lobos, "Testing black holes with cosmological constant in Einstein-bumblebee gravity through the black hole shadow using EHT data and deflection angle," 10 2024.
- [82] R. C. Pantig, "On the analytic generalization of particle deflection in the weak field regime and shadow size in light of EHT constraints for Schwarzschild-like black hole solutions," 8 2024.
- [83] H.-L. Li, M. Zhang, and Y.-M. Huang, "The shadows of quintessence non-singular black hole," *Eur. Phys. J. C*, vol. 84, no. 8, p. 860, 2024.
- [84] M. Khodadi, S. Vagnozzi, and J. T. Firouzjaee, "Event Horizon Telescope observations exclude compact objects in baseline mimetic gravity," *Sci. Rep.*, vol. 14, no. 1, p. 26932, 2024.
- [85] R. Ali, X. Tiecheng, R. Babar, and A. Ovgun, "Exploring light deflection and black hole shadows in Rastall theory with plasma effects," 2 2024.
- [86] Y. Meng, X.-M. Kuang, X.-J. Wang, B. Wang, and J.-P. Wu, "Images of hairy Reissner–Nordström black hole illuminated by static accretions," *Eur. Phys. J. C*, vol. 84, no. 3, p. 305, 2024.
- [87] N. Heidari, H. Hassanabadi, A. A. A. Filho, and J. Kríz, "Exploring non-commutativity as a perturbation in the Schwarzschild black hole: quasinormal modes, scattering, and shadows," *Eur. Phys. J. C*, vol. 84, no. 6, p. 566, 2024.
- [88] N. Heidari, H. Hassanabadi, A. A. A. Filho, J. Kríz, S. Zare, and P. J. Porfírio, "Gravitational signatures of a non-commutative stable black hole," *Phys. Dark Univ.*, vol. 43, p. 101382, 2024.
- [89] M. Calzà, D. Pedrotti, and S. Vagnozzi, "Primordial regular black holes as all the dark matter. II. Non-time-radial-symmetric and loop quantum gravity-inspired metrics," *Phys. Rev. D*, vol. 111, no. 2, p. 024010, 2025.
- [90] M. Calzà, D. Pedrotti, and S. Vagnozzi, "Primordial regular black holes as all the dark matter. I. Time-radial-symmetric metrics," *Phys. Rev. D*, vol. 111, no. 2, p. 024009, 2025.
- [91] V. Bozza, "Gravitational lensing in the strong field limit," *Phys. Rev. D*, vol. 66, p. 103001, 2002.
- [92] N. Tsukamoto, "Deflection angle in the strong deflection limit in a general asymptotically flat, static, spherically symmetric spacetime," *Phys. Rev. D*, vol. 95, no. 6, p. 064035, 2017.
- [93] N. Tsukamoto and Y. Gong, "Retrolensing by a charged black hole," *Phys. Rev. D*, vol. 95, no. 6, p. 064034, 2017.
- [94] Q.-M. Fu, L. Zhao, and Y.-X. Liu, "Weak deflection angle by electrically and magnetically charged black holes from nonlinear electrodynamics," *Phys. Rev. D*, vol. 104, no. 2, p. 024033, 2021.
- [95] S. H. Mazharimousavi, "Confinement and nonlinear electrodynamics: Asymptotic Schwarzschild charged black hole," *Phys. Dark Univ.*, vol. 43, p. 101413, 2024.
- [96] Z. Li, G. He, and T. Zhou, "Gravitational deflection of relativistic massive particles by wormholes," *Phys. Rev. D*, vol. 101, no. 4, p. 044001, 2020.
- [97] Z. Li, G. Zhang, and A. Övgün, "Circular Orbit of a Particle and Weak Gravitational Lensing," *Phys. Rev. D*, vol. 101, no. 12, p. 124058, 2020.
- [98] M. P. D. Carmo, *Differential Geometry of Curves and Surfaces*. New Jersey: Prentice-Hall, 1976.
- [99] Y. Huang, Z. Cao, and Z. Lu, "Generalized Gibbons-Werner method for stationary spacetimes," *JCAP*, vol. 01, p. 013, 2024.
- [100] E. Abbena, S. Salamon, and A. Gray, *Modern Differential Geometry of Curves and Surfaces with Mathematica*. Chapman and Hall/CRC, 3rd ed., 2006.
- [101] C. M. Will, *Theory and Experiment in Gravitational Physics*. Cambridge University Press, 9 2018.
- [102] M. L. Fil'chenkov and Y. P. Laptev, "Eddington's Prediction for General Relativity Revisited," *Grav. Cosmol.*, vol. 24, no. 4, pp. 371–374, 2018.
- [103] V. Perlick and O. Y. Tsupko, "Calculating black hole shadows: Review of analytical studies," *Phys. Rept.*, vol. 947, pp. 1–39, 2022.
- [104] V. Perlick, O. Y. Tsupko, and G. S. Bisnovatyi-Kogan, "Influence of a plasma on the shadow of a spherically symmetric black hole," *Phys. Rev. D*, vol. 92, no. 10, p. 104031, 2015.